# SUPPLEMENTARY INFORMATION

## Table of Contents

| | | |
|---|---|---|
| **Figure S12.** | The POLY_ANISO module analysis for **3** | |

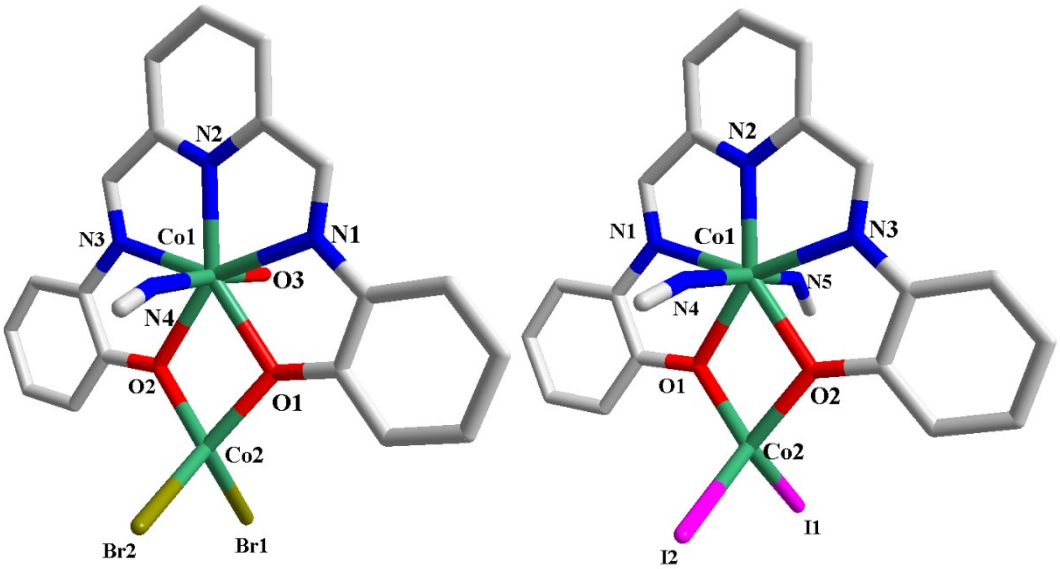


**Figure S1.** Representation of complexes **2** & **3** by wire or stick model.

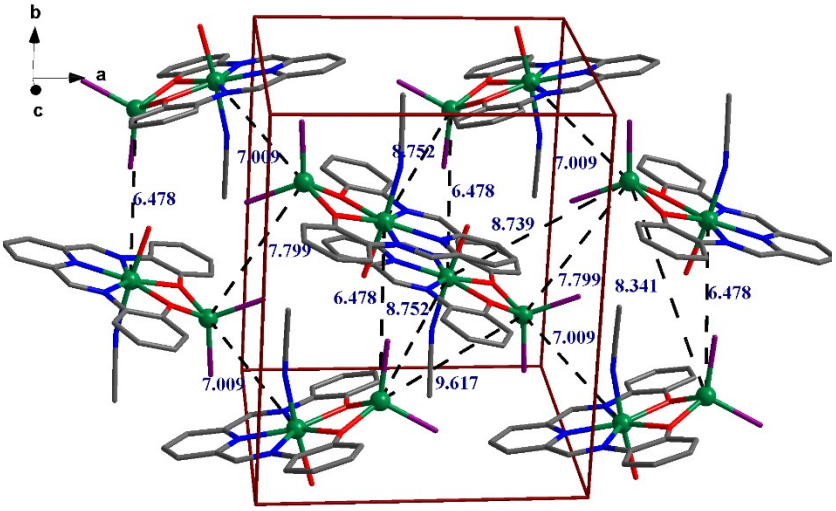

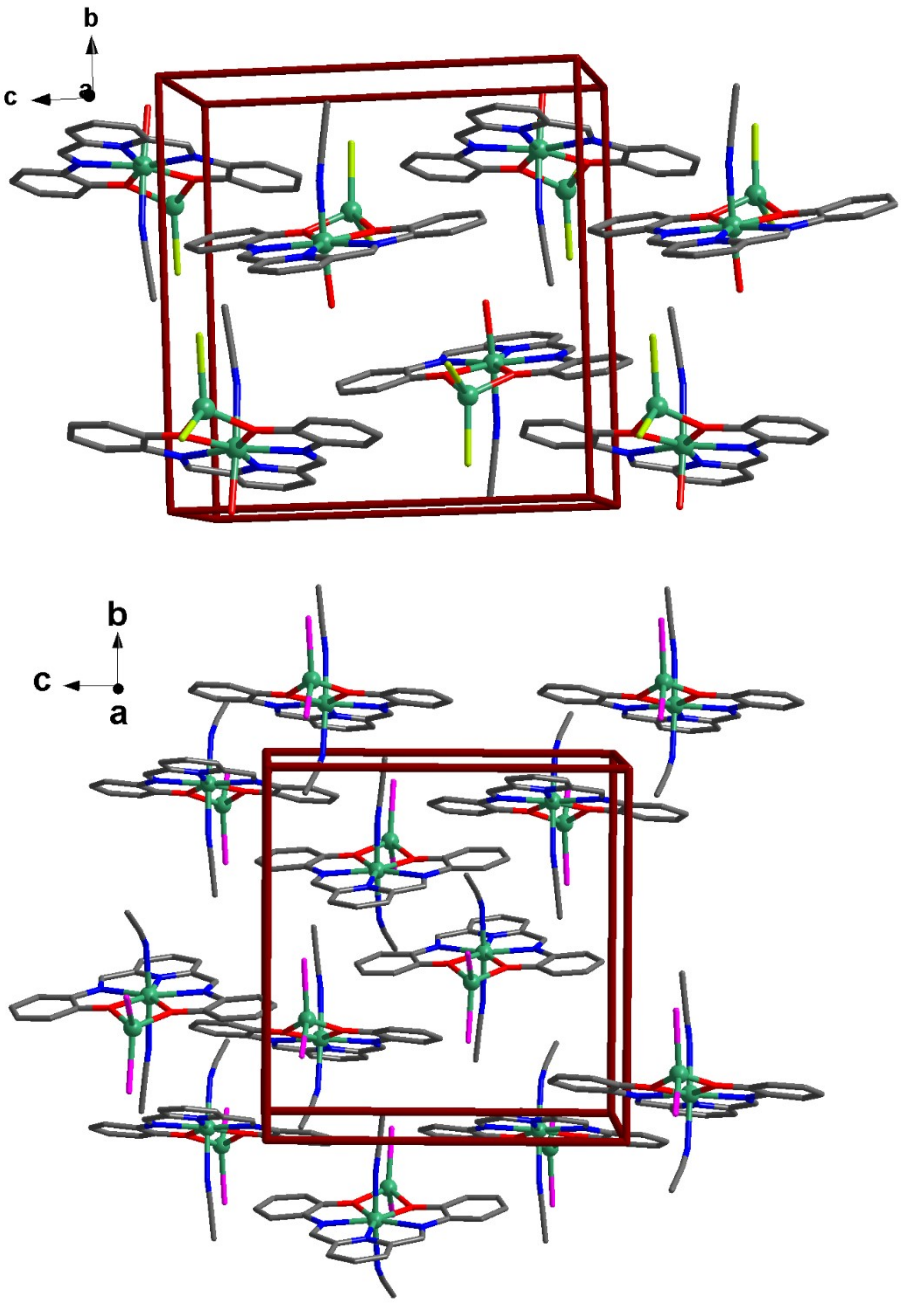


**Figure S2.** Packing diagram for complexes **1** (top), **2** (middle) and **3** (bottom).

**Table S1.** Crystal data and structure refinement parameters for complexes **1, 2** and **3**.

| | **1** | **2** | **3** |
|---|---|---|---|
| Empirical formula | $C_{21}H_{20}Cl_2Co_2N_4O_4$ | $C_{21}H_{20}Br_2Co_2N_4O_4$ | $C_{23}H_{19}I_2Co_2N_5O_2$ |
| Formula weight | 581.17 | 670.09 | 769.09 |
| Temperature/K | 273.15 | 105.0 | 298.0 |
| Crystal system | Monoclinic | Monoclinic | Monoclinic |

| Space group | $P2_1/n$ | $P2_1/n$ | $P2_1/n$ |
|---|---|---|---|
| $a$/Å | 12.068(3) | 12.3152(7) | 12.8418(7) |
| $b$/Å | 14.316(3) | 14.3406(8) | 14.6125(8) |
| $c$/Å | 13.869(3) | 13.8984(7) | 14.0835(8) |
| $\alpha$/° | 90 | 90 | 90 |
| $\beta$/° | 95.056(6) | 93.729(2) | 92.407(2) |
| $\gamma$/° | 90 | 90 | 90 |
| Volume/Å$^3$ | 2386.9(10) | 2449.4(2) | 2640.4(3) |
| $Z$ | 4 | 4 | 4 |
| $\rho_{calc}$g/cm$^3$ | 1.617 | 1.817 | 1.935 |
| $\mu$/mm$^{-1}$ | 1.649 | 14.732 | 3.624 |
| $F$(000) | 1716.0 | 1320.0 | 1472.0 |
| Crystal size/mm$^3$ | 0.076 × 0.055 × 0.043 | 0.4 × 0.2 × 0.18 | 0.16 × 0.15 × 0.14 |
| Radiation | MoK$_\alpha$ ($\lambda$ = 0.71073) | CuK$_\alpha$ ($\lambda$ = 1.54178) | MoK$_\alpha$ ($\lambda$ = 0.71073) |
| 2$\Theta$ range for data collection/° | 5.692 to 56.636 | 8.87 to 133.34 | 4.018 to 50.996 |
| Index ranges | $-16 \leq h \leq 16$, $-19 \leq k \leq 19$, $-18 \leq l \leq 18$ | $-14 \leq h \leq 14$, $-17 \leq k \leq 17$, $-16 \leq l \leq 16$ | $-15 \leq h \leq 15$, $-17 \leq k \leq 17$, $-17 \leq l \leq 17$ |
| Reflections collected | 37251 | 45670 | 62636 |
| Independent reflections | 5930 [$R_{int}$= 0.0542, $R_{sigma}$= 0.0346] | 4319 [$R_{int}$= 0.0648, $R_{sigma}$= 0.0351] | 4918 [$R_{int}$= 0.0465, $R_{sigma}$= 0.0202] |
| Data/restraints/parameters | 5930/0/303 | 4319/0/304 | 4918/11/309 |
| Goodness-of-fit on $F^2$ | 1.080 | 1.080 | 1.142 |
| Final $R$ indexes [$I$>=2$\sigma$ ($I$)] | $R_1$= 0.0345, | $R_1$= 0.0663, $wR_2$=0.1838 | $R_1$= 0.0824, |

| | | | |
|---|---|---|---|
| | $wR_2$=0.0801 | | $wR_2$=0.2556 |
| Final $R$ indexes [all data] | $R_1$= 0.0478, $wR_2$= 0.0894 | $R_1$= 0.0707, $wR_2$=0.1876 | $R_1$= 0.0952, $wR_2$= 0.2787 |
| Largest diff. peak/hole / e Å$^{-3}$ | 1.09/-0.94 | 1.24/-2.10 | 1.73/-2.90 |

**Table S2.** Comparison of bond lengths (Å) around $Co^{II}$ center in complexes **1**−**3.**

| Bond Length | **1** | **2** | **3** |
|---|---|---|---|
| Co1−$N_{imino}$ | 2.213(2) – 2.2239(19) | 2.217(5) – 2.219(5) | 2.218(7) – 2.219(7) |
| Co1−$N_{pyridine}$ | 2.145(2) | 2.141(5) | 2.132(8) |
| Co1−$O_{phenolate}$ | 2.1632(17) – 2.1676(17) | 2.164(4) – 2.165(5) | 2.150(7) – 2.159(6) |
| Co1-$N_{acetonitrile}$ | 2.134(2) | 2.134(6) | 2.162(9) – 2.177(11) |
| Co1-$O_{water}$ | 2.1742(18) | 2.179(5) | - |
| Co2−$O_{phenolate}$ | 1.9448(17) – 1.9522(16) | 1.937(4) – 1.938(4) | 1.931(6) – 1.943(6) |
| Co2−$X_{halogen}$ | 2.2536(9) – 2.2641(9) | 2.3285(14) - 2.3543(13) | 2.4240(19) – 2.5074(17) |
| $O_{phenolate}$-Co1-$O_{phenolate}$ | 70.16(6) | 70.26(16) | 70.8(2) |
| $O_{phenolate}$-Co2-$O_{phenolate}$ | 79.39(7) | 80.03(19) | 80.2(3) |
| $X_{halogen}$-Co2-$X_{halogen}$ | 110.71(3) | 110.47(6) | 115.91(7) |
| Co1-$O_{phenolate}$-Co2 | 103.67(7) | 103.53(19) | 103.9(3) |
| $N_{acetonitrile}$-Co1-$O_{water}$ | 175.57(8) | 176.0(2) | - |
| $N_{acetonitrile}$-Co1-$N_{acetonitrile}$ | - | - | 175.7(4) |

**Table S3:** BVS Calculations for the Co1 and Co2 centers.

| | **Co1-$N_{imino}$** | **Co1-$N_{imino}$** | **Co1-$N_{pyridine}$** | **Co1-$O_{phenolate}$** | **Co1-$O_{phenolate}$** | **Co1-$N_{acetonitrile}$** | **Co1-$N_{acetonitrile}$** | **Co1-$O_{water}$** | **Total BVS** |
|---|---|---|---|---|---|---|---|---|---|
| Bond Length **(1)** | 2.213 | 2.2239 | 2.145 | 2.1632 | 2.1676 | 2.134 | | 2.1742 | |
| BVS**(1)** | 0.243 | 0.236 | 0.295 | 0.279 | 0.276 | 0.301 | | 0.271 | 1.901 |
| Bond Length **(2)** | 2.217 | 2.219 | 2.141 | 2.164 | 2.165 | 2.134 | | 2.179 | |
| BVS **(2)** | 0.242 | 0.240 | 0.297 | 0.279 | 0.278 | 0.303 | | 0.268 | 1.907 |
| Bond | 2.218 | 2.219 | 2.132 | 2.150 | 2.159 | 2.162 | 2.163 | | |

| | | | | | | | | | |
|---|---|---|---|---|---|---|---|---|---|
| Length **(3)** | | | | | | | | | |
| BVS **(3)** | 0.241 | 0.240 | 0.304 | 0.290 | 0.281 | 0.280 | 0.280 | | 1.916 |

| | **Co2-$O_{phenolate}$** | **Co2-$O_{phenolate}$** | **Co2-X** | **Co2-X** | **Total BVS** |
|---|---|---|---|---|---|
| Bond Length **(1)** | 2.031 | 2.032 | 2.205 | 2.215 | |
| BVS **(1)** | 0.398 | 0.399 | 0.628 | 0.612 | 2.03 |
| Bond Length **(2)** | 2.0256 | 2.0478 | 2.193 | 2.212 | |
| BVS **(2)** | 0.406 | 0.382 | 0.649 | 0.616 | 2.05 |
| Bond Length **(3)** | 2.020 | 2.032 | 2.184 | 2.205 | |
| BVS **(3)** | 0.412 | 0.399 | 0.664 | 0.628 | 2.10 |

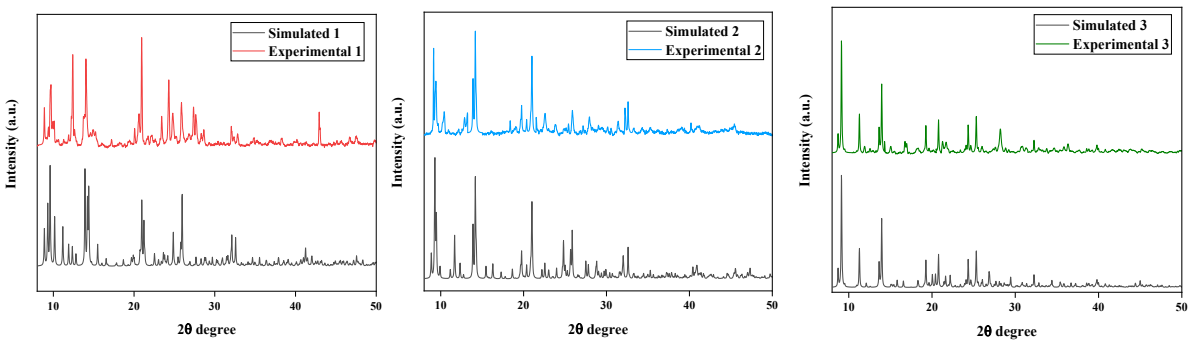


**Figure S3.** PXRD of Complexes **1 – 3**.

**Table S4**. Continuous Shape Measurements (*CShM*) for complexes **1**−**3**.

**<u>$Co_2Cl_2$</u>**

S H A P E  v2.0  Continuous Shape Measures calculation

(c) 2010  Electronic Structure Group, Universitat de Barcelona

Contact:  llunell@ub.edu

---

HP-7 1 D7h Heptagon

HPY-7 2 C6v Hexagonal pyramid

PBPY-7 3 D5h Pentagonal bipyramid

COC-7 4 C3v Capped octahedron

CTPR-7 5 C2v Capped trigonal prism

JPBPY-7 6 D5h Johnson pentagonal bipyramid J13

JETPY-7 7 C3v Johnson elongated triangular pyramid J7

| Structure [ML7] | HP-7 | HPY-7 | PBPY-7 | COC-7 | CTPR-7 | JPBPY-7 | JETPY-7 |
|---|---|---|---|---|---|---|---|
| vani , | 34.459, | 25.460, | 0.062, | 8.110, | 6.265, | 3.444, | 24.559 |

SP-4 1 D4h Square

T-4 2 Td Tetrahedron

SS-4 3 C2v Seesaw

| Structure [ML4 ] | SP-4 | T-4 | SS-4 |
|---|---|---|---|
| vani , | 26.881, | 3.567, | 9.360 |

**$Co_2Br_2$**

| Structure [ML7 ] | HP-7 | HPY-7 | PBPY-7 | COC-7 | CTPR-7 | JPBPY-7 | JETPY-7 |
|---|---|---|---|---|---|---|---|
| vani , | 34.824, | 25.575, | 0.056, | 8.107, | 6.339, | 3.470, | 24.621 |

| Structure [ML4 ] | SP-4 | T-4 | SS-4 |
|---|---|---|---|
| vani , | 28.113, | 3.749, | 10.111 |

**$Co_2I_2$**

Structure [ML7 ] HP-7 HPY-7 PBPY-7 COC-7 CTPR-7 JPBPY-7 JETPY-7

vani , 34.440, 25.739, 0.080, 8.155, 6.304, 3.639, 24.210

Structure [ML4 ] SP-4 T-4 SS-4

vani , 30.461, 4.290, 10.800

| Complex | HP-7 | HPY-7 | **PBPY-7** | COC-7 | CTPR-7 | JPBPY-7 | JETPY-7 |
|---|---|---|---|---|---|---|---|
| **$Co_2Cl_2$(Co1)** | 34.459 | 25.460 | **0.062** | 8.110 | 6.265 | 3.444 | 24.559 |
| **$Co_2Br_2$(Co1)** | 34.824 | 25.575 | **0.056** | 8.107 | 6.339 | 3.470 | 24.621 |
| **$Co_2I_2$(Co1)** | 34.440 | 25.739 | **0.080** | 8.155 | 6.304 | 3.639 | 24.210 |

| Complex | SP-4 | **T-4** | SS-4 |
|---|---|---|---|
| **$Co_2Cl_2$(Co2)** | 26.881 | **3.567** | 9.360 |
| **$Co_2Br_2$(Co2)** | 28.113 | **3.749** | 10.111 |
| **$Co_2I_2$(Co2)** | 30.461 | **4.290** | 10.800 |

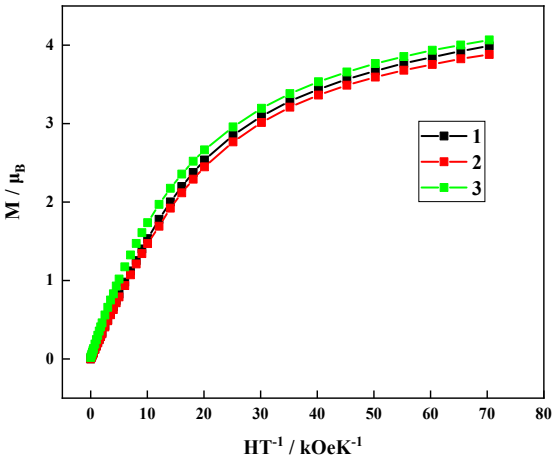


**Figure S4.** Field dependences of magnetization in the field range 0−70 kOe at 2 K temperature for **1−3**.

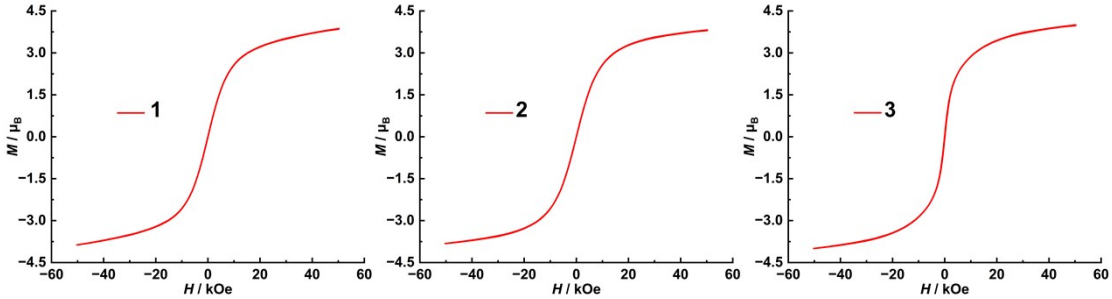


**Figure S5.** *M* (*H*) Hysteresis plots for **1**−**3** using a scan rate of 2.0 $mTs^{-1}$.

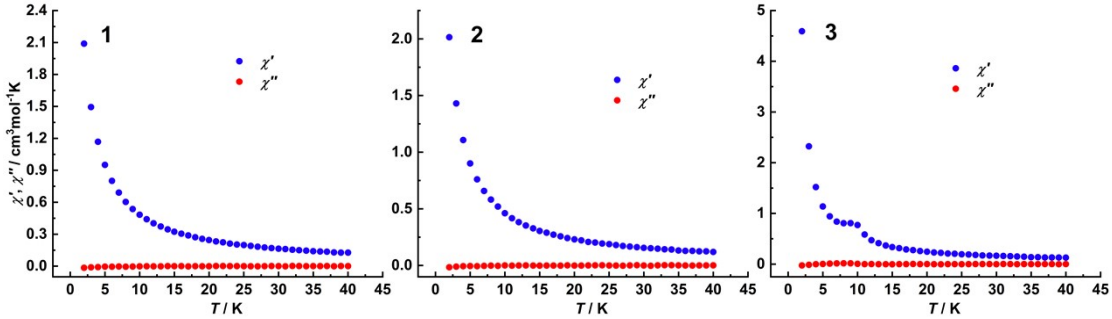


**Figure S6.** Plots of ac susceptibility vs. temperature at $H_{ac}$ = 3.5 Oe, $H_{dc}$ = 0 Oe, oscillating at 1−1488 Hz for **1**−**3**.

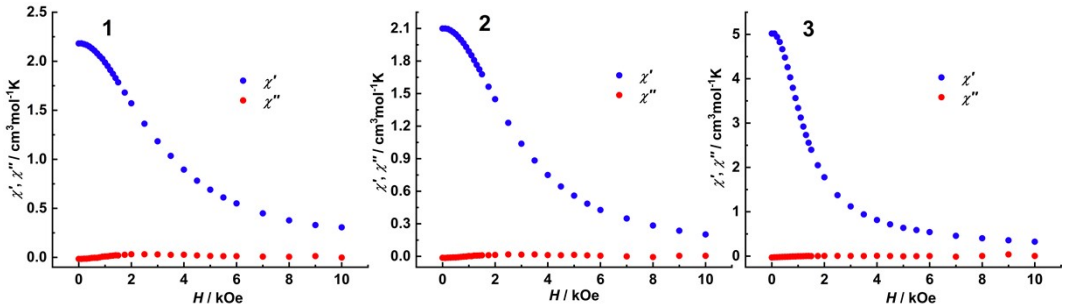


**Figure S7.** Plots of ac susceptibility vs. applied field from 0−10 kOe for **1**−**3**.

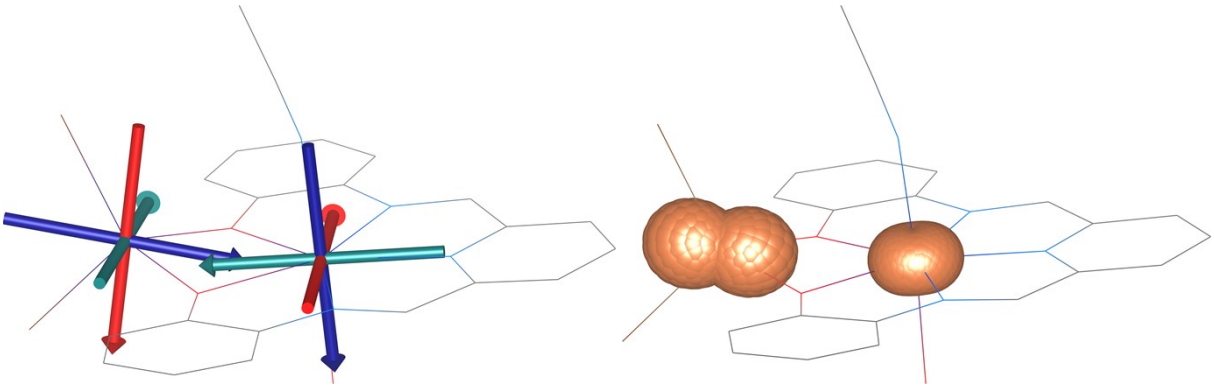

**Figure S8.** Molecular structure of **2** overlaid with a) *D*-tensors axes calculated with CASSCF/NEVPT2 (red/green/blue vectors represent x/y/z axes of D-tensors) on the left, b)

three-dimensional molar magnetization calculated at $T$ = 2 K and $B$ = 0.1 T on the right. The hydrogen atoms were omitted.

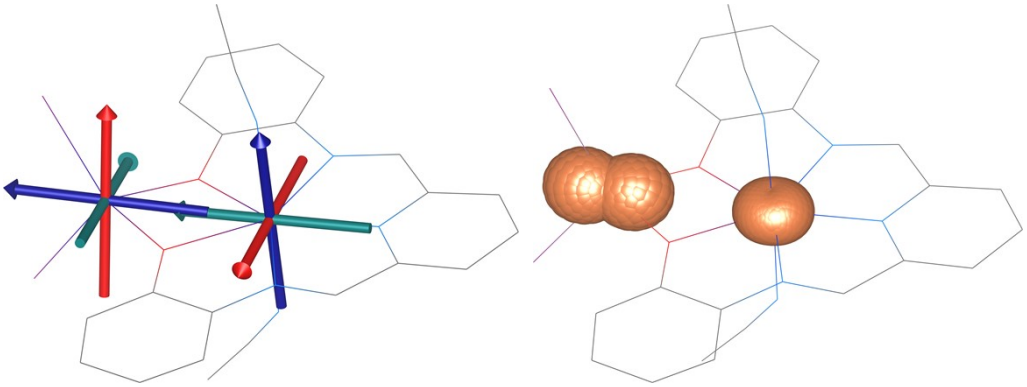

**Figure S9.** Molecular structure of **3** overlaid with a) $D$-tensors axes calculated with CASSCF/NEVPT2 (red/green/blue vectors represent x/y/z axes of D-tensors) on the left, b) three-dimensional molar magnetization calculated at $T$ = 2 K and B = 0.1 T on the right. The hydrogen atoms were omitted.

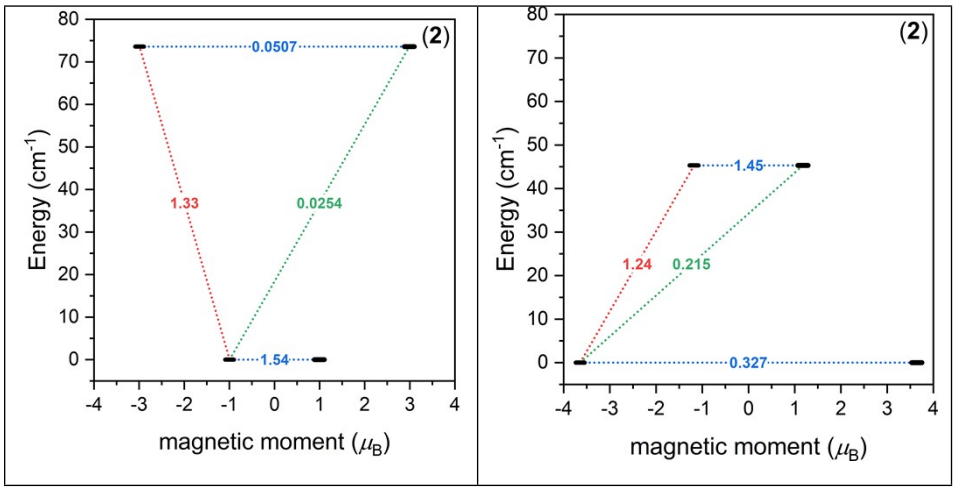

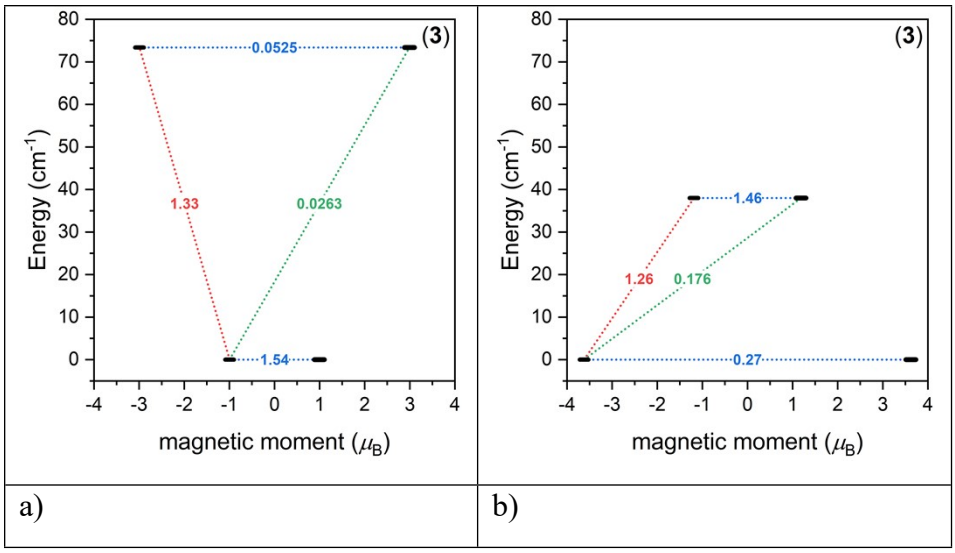


**Figure S10.** Magnetization reversal blocking barrier of pentagonal-bipyramidal $Co^{II}$ ion (a) and tetrahedral $Co^{II}$ ion (b) in **2-3** calculated by CASSCF/NEVPT2/SINGLE_ANISO. The numbers presented for the lowest two doublets represent the corresponding matrix element of the transversal magnetic moment (for values larger than 0.1, an efficient relaxation mechanism is expected).

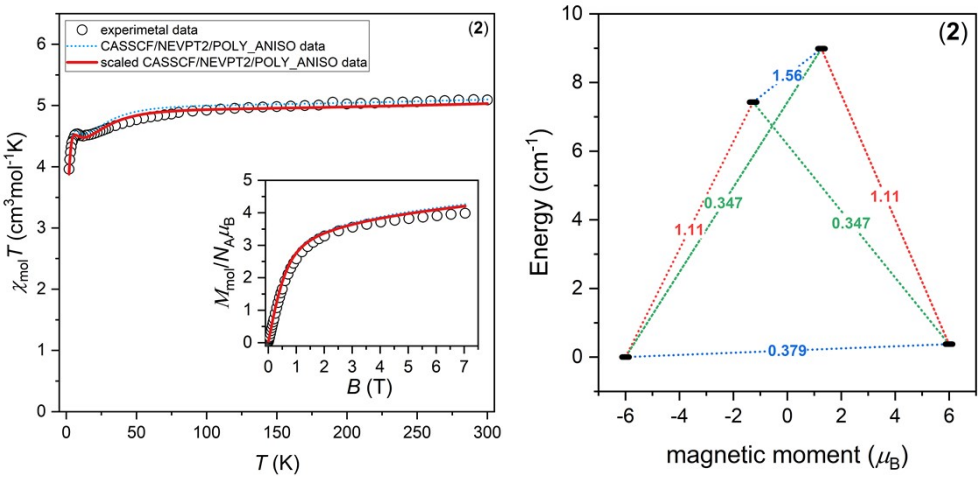


**Figure S11.** The POLY_ANISO module analysis for **2** with $J^{Lin} = 2.6$ cm$^{-1}$, $zj = -0.086$ cm$^{-1}$, and a scaling factor of 0.987. Left: temperature-dependent $\chi_{mol}T$ product and isothermal magnetization at $T = 1.9$ K. Right: magnetization reversal blocking barrier showing the two lowest pseudo-doublets. The values indicated for the two lowest doublets correspond to the corresponding matrix elements of the transversal magnetic moment. The values colored in blue show the tunneling gap $\Delta_{tun}$ (cm$^{-1}$) of the indicated pseudo-doublets.

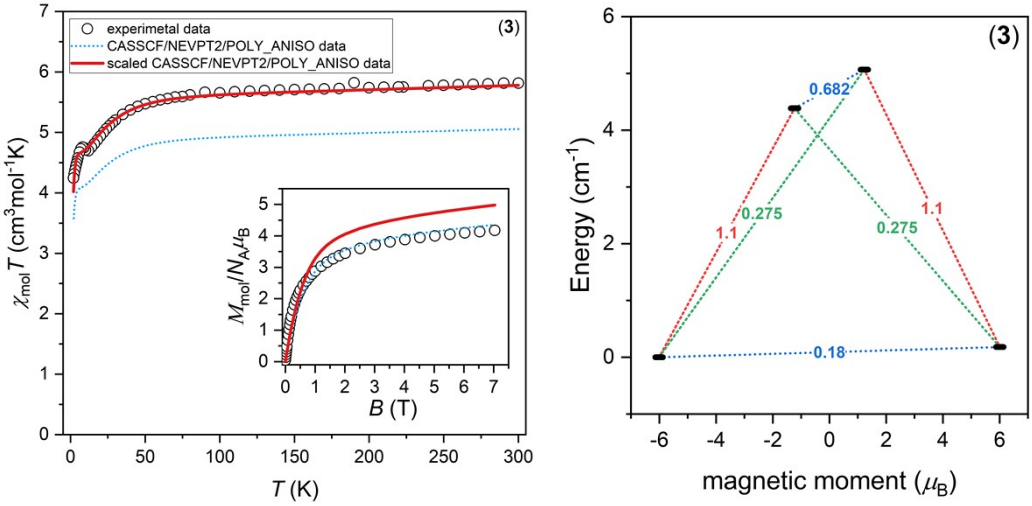


**Figure S12.** The POLY_ANISO module analysis for **3** with $J^{Lin}$ = 1.4 cm$^{-1}$, $zj$ = -0.14 cm$^{-1}$, and a scaling factor of 1.14. Left: temperature-dependent $\chi_{mol}T$ product and isothermal magnetization at $T$ = 1.9 K. Right: magnetization reversal blocking barrier showing the two lowest pseudo-doublets. The values indicated for the two lowest doublets correspond to the corresponding matrix elements of the transversal magnetic moment. The values colored in blue show the tunneling gap $\Delta_{tun}$ (cm$^{-1}$) of the indicated pseudo-doublets.